Chem. Res. Chin. Univ., 2015, 31(5), 846—850 doi: 10.1007/s40242-015-5019-0

Template Synthesis and Characterization of Cu_2O/TiO_2 Coaxial Nanocable for Photocatalysis

WANG Hongzhi, LIU Ning, LU Jing, YAO Suwei, JIANG Shisheng and ZHANG Weiguo*

Department of Applied Chemistry, School of Chemical Engineering and Technology, Tianjin University, Tianjin 300072, P. R. China

Abstract Coaxial nanocable consisted of p-type Cu_2O nanowires and n-type TiO_2 nanotubes arrays was prepared in the porous anodic aluminum oxide(AAO) template *via* the sol-gel method and subsequent electrodeposition method. X-ray diffraction analysis identified an anatase structure of the TiO_2 nanotubes and cubic structure of the Cu_2O nanowires. The obtained samples were also characterized by scanning electron microscopy(SEM), transmission electron microscopy(TEM) and energy dispersive X-ray spectroscopy(EDS). The diffrence of open circuit potential of the coaxial nanocable electrode was larger than that of the TiO_2 nanotubes electrode under ultraviolet illumination, which means doping with Cu_2O could improve the photovoltage effectively. Meanwhile, nanocable arrays exhibited a high activity for photodegrading Rhodamine B under Xe lamp irradiation and the photocatalysis degradation efficiency was up to 98.69% after degradation for 7 h. The enhanced photocatalytic activity could be attributed to the high migration efficiency of photoinduced electrons, which may suppress the charge recombination effectively.

Keywords TiO_2; Cu_2O; Coaxial nanocable; Heterojunction; Photocatalysis

1 Introduction

Recently, nanomaterials with one-dimensional structures, such as nanorods, nanotubes, and nanowires[1], have attracted considerable attention due to their excellent electronic, optical, catalytic, and mechanical properties[2—4]. One-dimensional nanomaterial can be synthesized by various methods such as vapor-phase approach, solvothermal synthesis and template synthesis methods[4—6]. Particular attention has been paid to template synthesis method using anodic aluminum oxide(AAO) because of its physical stability and chemical inertness.

TiO_2 is an n-type semiconductor with a wide band-gap energy of 3.2 eV and is famous for its excellent photocatalytic efficiency[5]. However, the poor utilization of solar energy and the high recombination rate of electron-hole pairs limit the photoelectrochemical properties of TiO_2. Therefore, coupling TiO_2 with narrow band gap semiconductors or other materials has been thought to be an efficient method to enhance the photocatalysis under visible light[6—13]. Cu_2O has a band-gap of 2.0—2.2 eV[14—17] and its high absorption coefficient in the visible region makes itself highly desirable in photochemistry[18,19].

In 1998, Hara *et al.*[20] discovered that Cu_2O exhibited a good catalytic performance and stability. The p-type cuprous oxide has recently been reported to be a good sensitizer to improve the photocatalytic activity of TiO_2 in solar energy utilization[21]. Zhang *et al.*[22] reported that the TiO_2/Cu_2O composite film exhibited better photocatalytic efficiencies than pure TiO_2 and Cu_2O under visible light irradiation. Hou *et al.*[23] found the method of depositing Cu_2O nanoparticles onto nanotubes by photoreduction deposition to prepare Cu_2O/TiO_2 heterojunction arrays.

In this study, we found a two-step route involving sol-gel and electrodeposition to fabricate Cu_2O/TiO_2 coaxial nanocable in the pores of AAO template, which was low cost and simplicity. Cu_2O/TiO_2 heterojunctions were successfully prepared, which were well-aligned and visible-light-active. The Cu_2O/TiO_2 heterojunctions showed high photodegradation efficiency of Rhodamine B under visible light irradiation. The different phenomena observed were discussed.

2 Experimental

2.1 Materials

All the reagents used in this work were of analytical grade that were used without any further purification. $(NH_4)_2TiF_6$, lactic acid and NaOH were purchased from Tianjin Guangfu Technology Development Co., Ltd., China; $CuSO_4·5H_2O$ was purchased from Sinopharm Chemical Reagent Co., Ltd., China; TiO_2(P25) was purchased from Degussa, Germany.

2.2 Preparation and Characterization of Cu_2O/TiO_2 Nanocable

2.2.1 Preparation of Cu_2O/TiO_2 Nanocable

AAO template was fabricated by a two-step anodization process as the method described in reference [16]. The pore diameter of AAO template was about 120 nm. Firstly, the

*Corresponding author. E-mail: zwg@tju.edu.cn

Received January 1, 2015; accepted March 23, 2015.

Supported by the Natural Science Foundation of Tianjin, China(No.11JCYBJC01900).

nanotubes were synthesized in the AAO template by sol-gel method. AAO template(1 cm×2 cm) was immersed in the solution of 0.1 mol/L $(NH_4)_2TiF_6$ at 30 °C for 1 h. Then, the template was taken out, rinsed with deionized(DI) water and dried in air at room temperature. Having been annealed at 300 °C for 2 h under N_2 atmosphere, the nanotubes were fabricated successfully inside AAO pores. A layer of Au film was sputtered onto one side of the TiO_2/AAO template served as the working electrode. Secondly, Cu_2O nanowires were electrodeposited on a TiO_2/AAO template electrode in a solution containing 0.4 mol/L $CuSO_4·5H_2O$ and 3 mol/L lactic acid. Electrodeposition was carried out at 60 °C, on a three-electrode potentiostatic system with a saturated calomel electrode(SCE) as a reference electrode and a platinum plate as a counter electrode. The deposition was carried out under potentiostatic conditions with a potential range of –0.2— –0.4 V. After the deposition, the sample was immediately rinsed with DI water and dried in air. Then, the coaxial nanocable of Cu_2O nanowires encapsulated in nanotubes was fabricated with the assistance of AAO template.

2.2.2 Characterization of Cu_2O/TiO_2 Nanocable

The morphologies of Cu_2O/TiO_2 nanocable were observed by scanning electron microscopy(SEM, S-4800, HITACHI, Japan), the detailed microscopic structure and chemical composition of the nanowires were characterized by transmission electron microscopy(TEM, JEM-2100, JEOL, Japan). The crystalline phase of Cu_2O/TiO_2 nanocable was established with an X-ray diffraction(XRD, 40 kV, 200 mA, Rigaku, Mutiflex, D/MAX-2500, Japan) under Cu *Kα* radiation. Besides, UV-visible absorption spectra of the samples were recorded on a spectrometer(TU-1901, PERSEE, China). Electrochemical experiments were performed at a model CHI 660B electrochemical workstation(Shanghai Chenhua Equipments, China). To obtain the specimen for SEM and TEM, the sample was dissolved in a 4 mol/L NaOH solution for 2 h at room temperature. Curves of open circuit potential(V_{oc}) were tested at electrochemical workstation on a three-electrode system under ultraviolet irradiation from a 100 W ultraviolet lamp(365 nm). Cu_2O/TiO_2 coaxial nanocable(2 cm×2 cm) served as the working electrode, while a platinum plate electrode and an SCE were used as the counter and reference electrodes respectively in separate compartment filled with an aqueous electrolyte solution of 0.5 mol/L Na_2SO_4. The diffrence of open circuit potential was calculated *via* $V_{oc}=|V_{light}-V_{dark}|$, where V_{light} is the potential when light was on and V_{dark} means the light was off. Photocatalytic degradation was carried with 0.3 g Cu_2O/TiO_2 coaxial nanocable in 100 mL of a 5 mg/L Rhodamine B solution under a 500 W Xe lamp(290—800 nm). Commercially available TiO_2(P25) was used as comparison. The degradation process was monitored by measuring the absorbance of the Rhodamine B solution at 554 nm on a spectrophotometer every 1 h. The photocatalysis degradation efficiency(D, %) was calculated by means of $D(\%)=(c_0-c)/c_0\times100\%$, where c_0 is the initial concentration of Rhodamine B in the solution; c the concentration of Rhodamine B at a given reaction time. To understand the semiconducting properties of as-deposited Cu_2O and TiO_2, Mott-Sckottky(MS) measurement was performed by virtue of the impedance technique. K_2SO_4 aqueous solution(0.2 mol/L) was chosen as the electrolyte solution. The MS plots were measured with an AC amplitude of 10 mV at a frequency of 1000 Hz in the dark.

3 Results and Discussion

3.1 Characterization of Cu_2O/TiO_2 Nanocable

3.1.1 Morphology of Cu_2O/TiO_2 Nanocable

Fig.1 shows the SEM images of AAO template, TiO_2 nanotubes, Cu_2O nanowires and Cu_2O/TiO_2 coaxial nanocables. In Fig.1(A), the pore diameter of AAO template is about 120 nm. From Fig.1(B) and (C), it can be clearly observed that the external diameter of the nanotubes is about 120 nm, which is the same as the pore diameter of AAO template. Cu_2O nanowires are distributed uniformly and the diameter is about 120 nm, too. Fig.1(D) and the inset show that the sample is abundant, uniform and highly ordered over a large area. The wall thickness of the nanotubes is 10 nm and the diameter of the Cu_2O nanowires is about 100 nm. The observations suggest that Cu_2O nanowires are compact and well attached to the inner walls of TiO_2 nanotubes, constructing the nanocable. All the above structure characterizations indicate that a promising Cu_2O/TiO_2 coaxial nanocable with well designed architecture has been constructed.

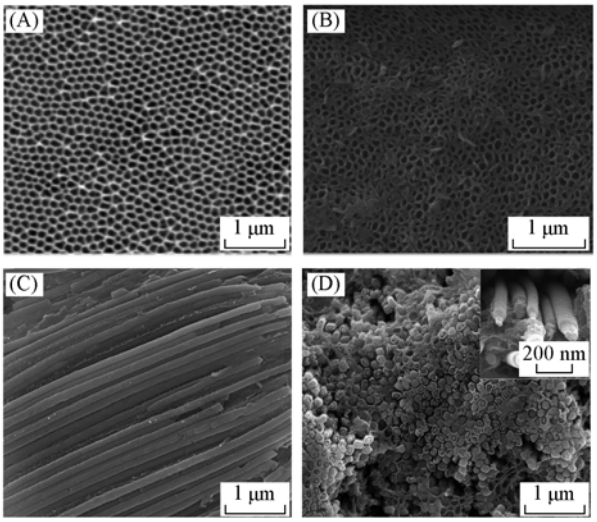

Fig.1 SEM images of AAO template(A), TiO_2 nanotubes(B), Cu_2O nanowires(C) and Cu_2O/TiO_2 coaxial nanocables(D)

Inset in (D) is the high magnification image of Cu_2O/TiO_2 coaxial nanocable.

Fig.2(A) is a TEM image of Cu_2O/TiO_2 coaxial nanocable(AAO template has been removed). The diameters of the Cu_2O nanowires and TiO_2 nanotubes are about 100 and 120 nm, respectively, which are in agreement with the SEM observation[Fig.1(D)]. It can also be seen that the TiO_2 nanotubes and Cu_2O nanowires are straight and have uniform thickness along the nanowires. The thickness of the tube wall is approximate 10 nm. As expected, the X-ray energy dispersive(EDS) analysis of the Cu_2O/TiO_2 coaxial nanocable is shown in Fig.2(B), which indicates that the elemental composition of the coaxial nanocable is O, Ti, Cu. In order to confirm the sample

to be Cu_2O/TiO_2 coaxial nanocable, EDS line-scan analysis was performed along the line in high angle annular dark-field(HAADF) image[Fig.2(C)] to elucidate the elemental distribution across the Cu_2O/TiO_2 coaxial nanocable. Cu signals are mainly confined within the internal region, while Ti signals are found to exhibit along the coaxial nanocable. C signals are from the TEM grid coated with a carbon film. The results indicate that the TiO_2 shell covers the Cu_2O nanowires homogeneously to form a coaxial structure.

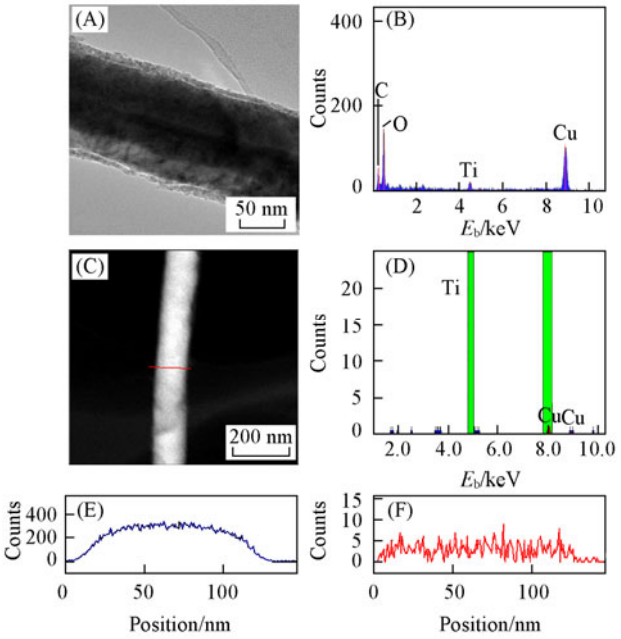

Fig.2 TEM image(A), EDS spectrum(B), HAADF image(C), EDS HAADF analysis(D), and variation of Cu(E) and Ti(F) of Cu_2O/TiO_2 coaxial nanocable

3.1.2 Crystal Properties of Cu_2O/TiO_2 Nanocable

Fig.3 shows the XRD pattern of Cu_2O/TiO_2 coaxial nanocable. The diffraction peaks of TiO_2 can be observed; the diffraction peaks at 2θ values of 25.28°, 37.80°, 48.05°, 55.06°, 62.69° and 75.03° can be perfectly indexed to (101), (004), (200), (211), (204) and (215) crystalline planes of anatase phase of TiO_2(JCPDS No. 21-1272) crystal, respectively. The diffraction peaks at 2θ values of 36.502°, 42.401°, 61.518° and 73.697° can be indexed to (111), (200), (220) and (311) crystalline planes of Cu_2O cubic phase(JCPDS No. 65-3288), respectively.

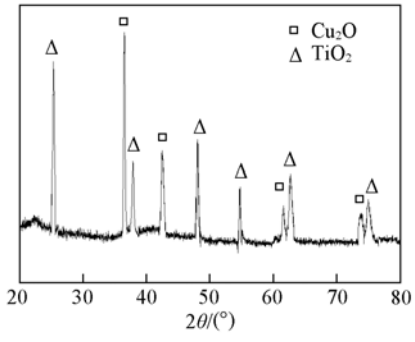

Fig.3 XRD pattern of Cu_2O/TiO_2 coaxial nanocable

3.2 Photoelectrochemical Performance

Fig.4 shows the open-circuit potential curves of pure TiO_2 nanotubes and Cu_2O/TiO_2 coaxial nanocable determined under dark or light. It can be found that Cu_2O/TiO_2 coaxial nanocable showed significant potential decrease when the light irradiated onto the sample. The V_{oc} is 308 mV, while V_{oc} of pure TiO_2 nanotubes is only 147 mV, which is much lower than that of the coaxial nanocable. As Cu_2O is a p-type semiconductor and TiO_2 is an n-type semiconductor, they compose p-n heterojunction on the interface. With the UV light irradiation, the photogenerated carriers on p-n heterojunction will be separated and their recombination rate will be depressed. That means TiO_2 doped with Cu_2O exhibits a great utilization rate of solar energy.

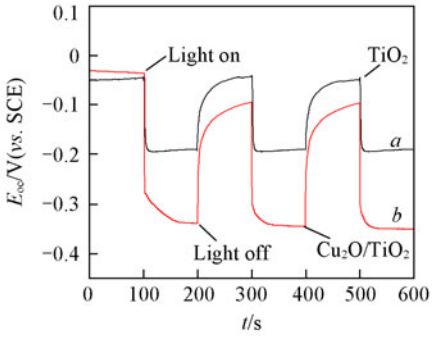

Fig.4 Open-circuit potential curves of pure TiO_2 nanotubes(*a*) and Cu_2O/TiO_2 coaxial nanocable(*b*) electrodes

3.3 Photocatalytic Activities

Fig.5 shows the degradation rate of Rhodamine B catalyzed by Cu_2O/TiO_2 coaxial nanocable, TiO_2 nanotubes, TiO_2(P25) and without catalyst under the Xe lamp irradiation. The degradation rate of Rhodamine B is only 11.17% without catalyst after irradiation for 7 h, which indicates Rhodamine B solution is stable under this condition. After irradiation for 4 h, the degradation rates of Rhodamine B are 36.89% and 94.30% in the presence of pure TiO_2 nanotubes and Cu_2O/TiO_2 coaxial nano- cable respectively. After irradiation for 7 h, the degradation rates of Rhodamine B have been increased to 49.77% and 98.69% in the presence of pure TiO_2 nanotubes and Cu_2O/TiO_2 coaxial nanocable, respectively. The degradation rate of

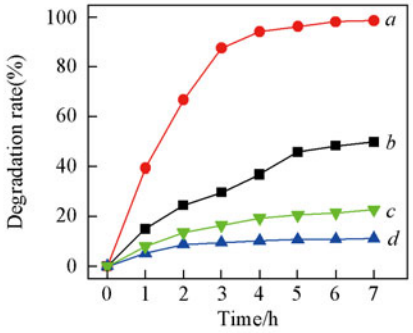

Fig.5 Degradation curves of Rhodamine B catalyzed by Cu_2O/TiO_2 coaxial nanocable(*a*), TiO_2 nanotubes(*b*), TiO_2(P25)(*c*) and without catalyst(*d*)

Rhodamine B in the presence of pure TiO_2 nanotubes is about two times that in the presence of pure TiO_2(P25). Experimental results show that Cu_2O/TiO_2 coaxial nanocable has much better photocatalytic activity than pure TiO_2 nanotubes.

Fig.6 shows the results of the fitted curves of the degradation efficiency of Cu_2O/TiO_2 coaxial nanocable, TiO_2 nanotubes, or TiO_2-P25 in the first 4 h. The degradation reaction of Rhodamine B can be described as a pseudo-first-order reaction with the kinetics expressed by the following equation when the Rhodamine B concentration is low(<1 mmol/L): $\ln(c_0/c)=kt$, where c_0 and c are the same meaning as those described before; t and k are the reaction time and the kinetics constant. The kinetics constant and the correlation coefficient of photocatalytic reactions are listed in Table 1.

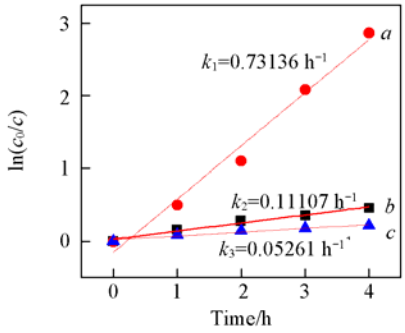

Fig.6 Variation of $\ln(c_0/c)$ with degradation time in photocatalytic processes in the presence of Cu_2O/TiO_2 coaxial nanocable(*a*), TiO_2 nanotubes(*b*) or TiO_2(P25)(*c*)

Table 1 Apparent rate constants and correlation coefficients of Rhodamine B solutions

Catalyst	Kinetics constant, k/h^{-1}	Correlation coefficient, R
Cu_2O/TiO_2 coaxial nanocable	0.73136	0.98964
TiO_2 nanotubes	0.11107	0.99224
TiO_2(P25)	0.05261	0.96356

The studied photocatalysis degradation obey the first-order kinetics with the apparent rate constants calculated from the plot of relative concentration *vs*. time shown in Fig.6. The determined reaction kinetics constants(k) were 0.73136, 0.11107 or 0.05261 h^{-1} respectively, in the presence of Cu_2O/TiO_2 coaxial nanocable, TiO_2 nanotubes or TiO_2(P25). The degradation rate of Rhodamine B is faster when the TiO_2 has been modified with Cu_2O. As there is always a p-n heterojunction in the Cu_2O/TiO_2 nanocable, photogenerated charges are separated easily. As a result, the rate of the recombination of the hole and electron decreased and more active oxidizing radical species thereby formed, which promotes the faster decomposition.

3.4 Mechanism of Photocatalytic Activity Enhancement

Fig.7 shows the evolution of absorbance *vs*. the incident wavelength for pure Cu_2O nanowires, TiO_2 nanotubes prepared and TiO_2(P25). According to the spectra, TiO_2 nanotubes present its characteristic absorption sharp edge rising at 387 nm, while Cu_2O nanowires absorb the light up to a wavelength of 650 nm. The band gaps(E_g) of TiO_2 and Cu_2O can be estimated[8] to be about 3.20 and 1.91 eV respectively from the onset of the absorption edge. Obviously, doping Cu_2O will increase the absorption in the visible light region.

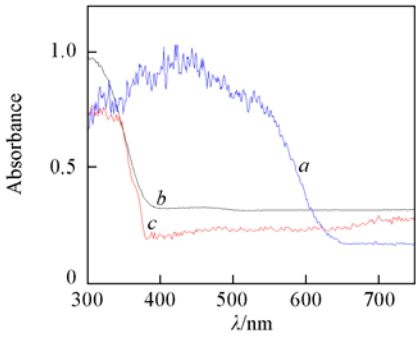

Fig.7 UV-Vis absorption spectra of Cu_2O nanowires(*a*), TiO_2 nanotubes(*b*) and TiO_2(P25)(*c*)

Fig.8 shows the MS plots of pure Cu_2O nanowires and TiO_2 nanotubes synthesized directly into AAO template. The positive slope of the plot in the linear region indicates an n-type semiconductor according to MS relationships on n-type semiconductors, and the negative slope line suggests p-type behavior on the basis of MS relationships on p-type semiconductors[24]. Thus, as-deposited Cu_2O nanowires and TiO_2 nanotubes exhibit p-type and n-type conductivity, respectively. The flat potential(V_{fb}) of TiO_2, as calculated from the x intercept of the linear region, was found to be –0.55 V *vs*. SCE[equivalent to –0.31 V *vs*. the normal hydrogen electrode(NHE)]. It is generally known that the conduction band potential(E_{CB}) of n-type semiconductor is very close to(0—0.2 V more negative) the V_{fb}[25]. Here, the difference between the conduction band potential and the flat potential is set to 0.1 V. Thus, the negative shift causes the E_{CB} shift of TiO_2 from –0.31 V to –0.41 V *vs*. NHE. Because the conduction band[26] at pH 7 for Cu_2O is –1.54 eV

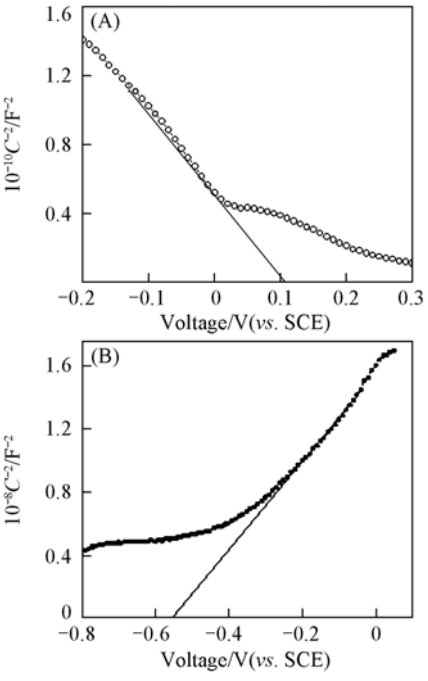

Fig.8 Mott-Schottky plots of Cu_2O nanowires(A) and TiO_2 nanotubes(B)

vs. NHE. This value is more negative than the conduction band potential of TiO_2. In this case, thermodynamic conditions favor the electron transfer from Cu_2O to TiO_2 when they are in contact. The Cu_2O/TiO_2 nanocable made into the template has high orientation and large p-n heterojunction interface area, which is in favor of charge transfer between interfaces. Based on the above results, the photocatalytic activity enhancement could be attributed to the high migration efficiency of photo induced electrons. The higher conduction band position of Cu_2O indicates a stronger reductive power, which may be effectively involved in the oxygen reduction reaction. Meanwhile, Cu_2O with a p-type structure could efficiently transfer the photogenerated electrons from E_{CB} of Cu_2O to that of TiO_2. Thus, in Cu_2O/TiO_2 nanocable, TiO_2 served as an acceptor of the generated electrons and effectively suppressed the charge recombination, leaving more hole charge carriers and promoting the degradation. This mechanism of the enhancement of the photocatalytic activity is summarized and illustrated in Fig.9.

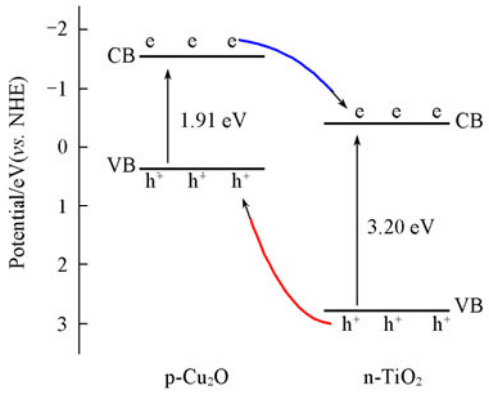

Fig.9 Band alignment for the heterostructures of Cu_2O/TiO_2

4 Conclusions

We successfully fabricated n-type TiO_2 and p-type Cu_2O to prepare Cu_2O/TiO_2 coaxial nanocable for photocatalysis by combinating sol-gel method with electrodeposition method with the aid of AAO template. We found that the Cu_2O/TiO_2 coaxial nanocable was highly ordered and Cu_2O nanowires wrapped tightly in TiO_2 nanotubes according to TEM, SEM and EDS observations. XRD pattern indicated that Cu_2O/TiO_2 coaxial nanocable was formed. Photoelectrochemical and photocatalytic performance showed the Cu_2O/TiO_2 coaxial nanocable had better activities than the pure TiO_2 nanotubes. Doping Cu_2O could effectively improve the degradation and photoelectric response property of TiO_2. The enhanced photocatalytic activity was due to the high migration efficiency of photoinduced electrons and reduced charge recombination efficiency.

References

[1] Subarna B., Susanta K. M., Prajna P. D., Mano M., *Chem. Mater.*, **2008**, *20*(21), 6784
[2] Xi Y. Y., Zhou J. Z., Guo H. H., *Chem. Phys. Lett.*, **2005**, *412*(1), 60
[3] Lu X. F., Mao H., Zhang W. J., *Nanotechnology*, **2007**, *18*(2), 025604
[4] He X. Z., Quan X. Z., Zhang X., *Appl. Phys. Lett.*, **2003**, *83*(9), 1689
[5] Feng Y., Yin J. H., Chen M. H., Song M. X., Su B., Lei Q. Q., *Mater. Lett.*, **2013**, *96*, 113
[6] Ke C., Cai F. G., Yang F., Cheng C. H., Zhao Y., *Chem. J. Chinese Universities*, **2013**, *34*(2), 423
[7] Zhou W., Yin Z., Du Y., Huang X., Zeng Z., Fan Z., Liu H., Wang J., Zhang H., *Small*, **2013**, *9*(1), 140
[8] Yuan J. J., Li H. D., Wang Q. L., Cheng S. H., Zhang X. K., Yu H. J., Zhu X. R., Xie Y. M., *Chem. Res. Chinese Universities*, **2014**, *30*(1), 18
[9] Tang Y. W., Chen Z. J., Jia Z. J., Zhang L. S., Li J. L., *Mater. Lett.*, **2005**, *59*(4), 434
[10] Liu Y., Ji H. W., Zhou D. F., Zhu X. F., Li Z. H., *Chem. J. Chinese Universities*, **2014**, *35*(1), 19
[11] Tan Y. W., Xue X. Y., Peng Q., Zhao H., Wang T. H., Li Y. D., *Nano Letters*, **2007**, *7*(12), 3723
[12] Zhang Z., Chen A. P., Ma L., He H. B., Li C. Z., *Chem. J. Chinese Universities*, **2013**, *34*(3), 656
[13] Liu Y., Yu L., Wei Z. G., Pan Z. C., Zou Y. D., Xie Y. H., *Chem. J. Chinese Universities*, **2013**, *34*(2), 434
[14] Du S. S., Cheng P. F., Sun P., Wang B., Cai Y. X., Liu F. M., Zheng J., Lu G. Y., *Chem. Res. Chinese Universities*, **2014**, *30*(4), 661
[15] De Jongh P. E., Vanmaekelbergh D., Kelly J. J., *Chem. Mater.*, **1999**, *11*(12), 3512
[16] Xiao H., Ai Z., Zhang L., *J. Phy. Chem. C*, **2009**, *113*(38), 16625
[17] Hao Y. Z., Sun B., Luo C., Fan L. X., Pei J., Li Y. P., *Chem. J. Chinese Universities*, **2014**, *35*(1), 127
[18] Lin P., Chen X., Yan X., Zhang Z., Yuan H., Li P., Zhao Y., Zhang Y., *Nano Research*, **2014**, *7*(6), 860
[19] Zheng Z. K., Huang B. B., Wang Z. Y., Guo M., Qin X. Y., Zhang X. Y., *J. Mater. Chem.*, **2011**, *21*(25), 9079
[20] Michikazu H., Takeshi K., Mutsuko K., Sigeru I., Kiyoaki S., Akira T., Junko N., Kazunari D., *Chem. Commun.*, **1998**, (3), 357
[21] Nageh K. Allam, Craig A. Grimes, *Mater. Lett.*, **2011**, *65*(12), 1949
[22] Zhang Y. G., Ma L. L., Li J. L., Yu Y., *Environm. Sci. Technol.*, **2007**, *41*(17), 6264
[23] Hou Y., Li X. Y., Zhou X. J., Quan X., Chen G. H., *Appl. Phys. Lett.*, **2009**, *95*(9), 093108
[24] Zhuang P. Q., Xiao Z. W., Zhu X. D., *Electronic Components and Materials*, **2011**, *30*(8), 35
[25] Bessekhouad Y., Robert D., Weber J. V., *Catalysis Today*, **2005**, *101*(3), 315
[26] Kramm B., Laufer A., Reppin D., Kronenberger P., Hering A., *Appl. Phys. Lett.*, **2012**, *100*(9), 094102